Contamination of silicon by iron at temperatures below 800 °C

J. D. Murphy[*, 1] **and R. J. Falster**[**, 1, 2]

[1] Department of Materials, University of Oxford, Parks Road, Oxford, OX1 3PH, UK
[2] MEMC Electronic Materials, viale Gherzi 31, 28100 Novara, Italy

[*] Corresponding author: e-mail john.murphy@materials.ox.ac.uk, Phone: +44 1865 273746
[**] e-mail rfalster@memc.it

Iron-related defects are deleterious in silicon-based integrated circuits and photovoltaics, ruining devices and acting as strong recombination centres. Unless great care is taken, iron contamination will result from high temperature processing and so it is essential to understand the degree to which this can occur. Iron solubility data above ~800 °C have been summarised by Istratov et al. (Appl. Phys. A **69**, 13 (1999)), but many processes are performed at lower temperatures for which solubility data are scarce. We have studied iron contamination below ~800 °C. Iron concentrations in intentionally contaminated air-annealed Czochralski silicon samples were determined from the change in minority carrier lifetime due to photodissociation of FeB pairs measured by quasi-steady-state photoconductance. In the ~600 to 800 °C temperature range the iron concentration was found to vary according to $1.3 \times 10^{21} \exp\left(-\dfrac{1.8\,\text{eV}}{kT}\right) \text{cm}^{-3}$. It is therefore the case that significantly more iron can dissolve in silicon at these temperatures than extrapolation of higher temperature data suggests, with the enhancement being by a factor of >20 at 600 °C.

1 Introduction Avoiding contamination of silicon by metallic impurities is a major issue for both integrated circuit (IC) [1] and photovoltaic [2] applications. Iron-related defects are recognised to have particularly harmful effects, including ruining electronic devices [3], acting as strong recombination centres [4] and forming precipitates which cannot easily be gettered [5]. There is a desire to use increasingly less pure material for multicrystalline silicon solar cells [6], so improving on ways to deal with iron contamination is of high importance.

The solubility of an impurity is a key parameter underpinning any process used to getter it. Processes such as phosphorus diffusion gettering and aluminium gettering rely on higher impurity solubility in the gettering layer compared to in the silicon [7]. Another approach is to use long low temperature (~500 to 700 °C) anneals to redistribute impurities to regions where they are less detrimental to minority carrier lifetime [8, 9]. This requires a delicate balance between low solubility (to prevent further contamination) and sufficiently high diffusivity, and studies have shown improvements in lifetime [8] and cell efficiency [9].

To improve both these gettering methods it is first necessary to know the solubility of iron in silicon itself.

At high temperatures the solubility of iron in silicon has been thoroughly studied. Results from experiments on intentionally contaminated samples have been consolidated into a single expression, which is valid above 800 °C and below the eutectic at ~1200 °C [10]:

$$S_{\text{high}} = 8.4 \times 10^{25} \exp\left(-\frac{2.86\,\text{eV}}{kT}\right) \text{cm}^{-3} . \qquad (1)$$

However, processes are often performed at temperatures below 800 °C. As well as the long low temperature gettering anneals [8, 9], annealing at ~650 °C is routinely used in IC silicon to annihilate thermal donor defects [11]. It is therefore vital to understand how much iron can dissolve in silicon at these lower temperatures too, and this is the subject of this Letter.

Iron is usually incorporated into silicon in interstitial form (Fe$_i$) [10]. At room temperature positively charged Fe$_i$ is mobile and it will interact with negatively charged substitutional boron to form FeB pairs. These FeB pairs

can be dissociated by light and the change in minority carrier lifetime that occurs is the established method for iron concentration measurement [4, 12] used in this study.

2 Experimental methods High-purity boron doped Czochralski silicon wafers (~2 to ~17 Ω cm) were cleaved into ~5 cm by 5 cm squares. Iron was put on the back (unpolished) side of each sample, by either rubbing the sample with iron pieces (99.95% purity from Testbourne Limited, UK) or by evaporation of iron wire (99.95% purity from Goodfellow Cambridge Limited, UK). Specimens were annealed in air in a pre-heated furnace at temperatures from 526 to 897 °C. Annealing times were considerably greater than the time required for iron to diffuse through the thickness of the sample according to well-established diffusivity values [10]. Samples were rapidly cooled to room temperature to quench in the iron concentration and to prevent iron precipitation. They were then subjected to an HF dip followed by an RCA clean. The sample surfaces were both passivated with silicon nitride grown by plasma enhanced chemical vapour deposition. This was done in either a direct plasma system at 350 °C (the majority of samples) or a remote plasma system at 400 °C.

Minority carrier lifetime was measured at room temperature by quasi-steady-state photoconductance (QSS-PC) [13] using a Sinton WCT-120 lifetime tester. Before testing samples were placed on a hotplate at 200 °C for 10 minutes to eliminate any effects related to boron–oxygen defects. To dissociate FeB pairs, 50 flashes with a ~10 μs decay constant from a Quantum Qpaq-X flash lamp placed very close to the sample were used. An initial lifetime measurement was made immediately. A final lifetime measurement was made at least 24 hours later, which for the conditions investigated is sufficient time for complete reassociation of the FeB defect [14].

3 Results
3.1 Identification of iron Minority carrier lifetime curves for contaminated samples annealed at 674 °C and 733 °C are shown in Fig. 1. The initial measurement was made with the vast majority of iron in the Fe_i state and the final measurement was made with the iron in the FeB state. The injection dependences of the two lifetime curves are typical of the interstitial iron defect and the iron–boron pair, and the cross-over characteristic of iron is observed [4]. The absolute value of lifetime is affected by other recombination mechanisms (including surface recombination, recombination at other defects and intrinsic mechanisms). However, as the intense illumination only alters the iron state, the difference between the initial and final (reciprocal) lifetimes can be used accurately to determine the iron concentration regardless of other recombination in the samples [4, 12]. The change in lifetime was fitted with Shockley–Read–Hall statistics using the recombination parameters of Rein and Glunz [4] with the total iron concentration as the variable parameter. Details of this fitting are given elsewhere [15]. It is noted that QSS-PC can be
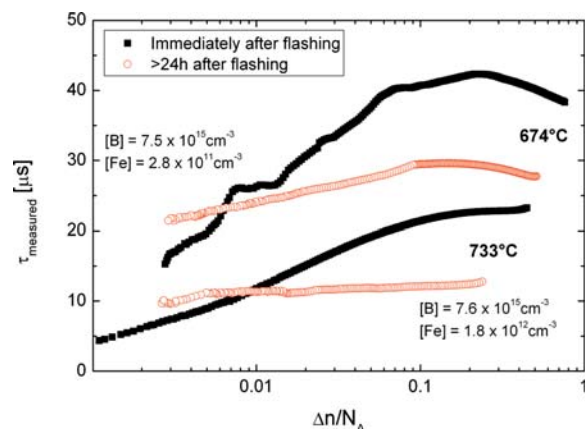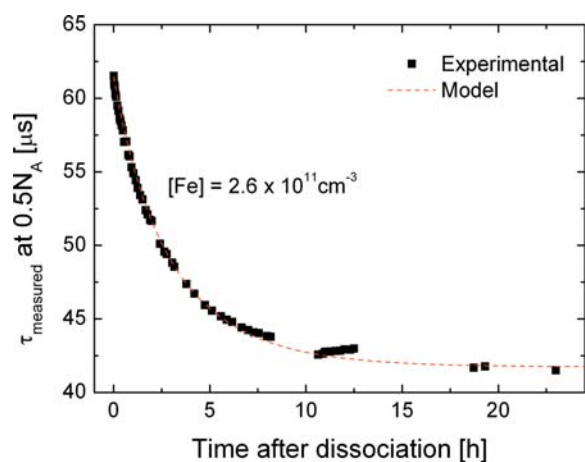

Figure 1 (online colour at: www.pss-rapid.com) Minority carrier lifetime ($\tau_{measured}$) as a function of excess carrier concentration (Δn) normalised by the doping level (N_A) for samples contaminated at two different temperatures.

more sensitive to lower iron concentrations than the surface photovoltage technique used in most of the previous work [10] as it can provide higher levels of injection for which the lifetime difference between Fe_i and FeB is greater.

Figure 2 shows lifetime at an injection level of $0.5N_A$ versus time after dissociation of the FeB pairs in a sample contaminated at 656 °C. The experimental results are very well described by a model based on the kinetics of iron diffusion and the binding energy of the FeB defect [14] described elsewhere [15]. This confirms that the intense illumination acts only to dissociate the FeB defect.

3.2 Iron contamination as a function of temperature Iron concentrations measured in samples contaminated at different temperatures are plotted in Fig. 3.

Figure 2 (online colour at: www.pss-rapid.com) $\tau_{measured}$ at $0.5N_A$ versus time after dissociation of FeB pairs in a sample contaminated at 656 °C. The experimental data are in excellent agreement with the reassociation kinetics [14, 15].

The level of injection generally used for the iron concentration determination was $0.2N_A$. This was chosen to minimise the error in measurement (it lies far from the cross-over) and because the level could be achieved even in most samples contaminated at the highest temperatures (lowest lifetimes). An extrapolation of the iron solubility found at higher temperatures given by Eq. (1) is also plotted. At temperatures of ~ 850 °C and above, the iron concentrations measured in this study are consistent with previous work [10]. Below this temperature, we find substantial deviation from that expected from extrapolation of Eq. (1). Between ~ 600 and 800 °C the iron concentration was found to vary according to

$$S_{\text{low}} = 1.3 \times 10^{21} \exp\left(-\frac{1.8 \text{ eV}}{kT}\right) \text{cm}^{-3} . \qquad (2)$$

Considering the scatter in the experimental data, the precision of the activation energy is ± 0.1 eV and that of the pre-factor is a factor of ± 2.

Below ~ 600 °C, the iron concentration is approximately constant at $\sim 8 \times 10^{10}$ cm^{-3}. It is noted that this is comfortably above the measurement limit of QSS-PC. It is also noted that samples pre-annealed at 720 °C for 24 h prior to being slow cooled to 550 °C have iron concentrations below $\sim 8 \times 10^{10}$ cm^{-3} in approximate agreement with an extrapolation of Eq. (2).

4 Discussion The results presented in Fig. 3 show that the concentration of iron that can be incorporated into silicon at temperatures below ~ 800 °C is substantially higher than given by extrapolation of Eq. (1). The enhancement is by a factor of ~ 5 at 700 °C, ~ 11 at 650 °C and ~ 22 at 600 °C. An enhancement in iron solubility has previously been observed in highly boron doped silicon due to Fermi level effects [16], but this cannot explain our results as the material is intrinsic at all contamination temperatures used. The fact that pre-annealing at 750 °C can affect the iron

contamination level of samples subsequently annealed below 600 °C suggests that different phases of iron silicide are formed in the different temperature ranges.
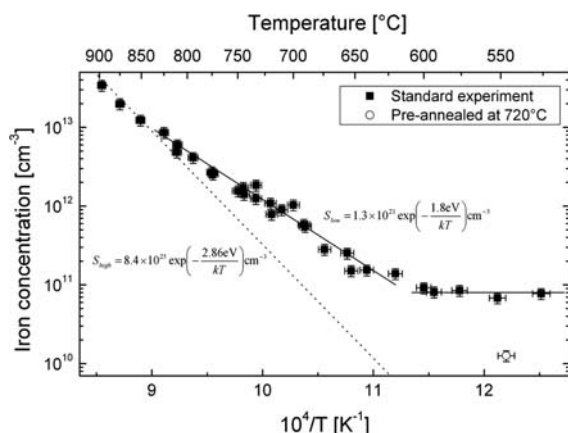
It is known empirically that iron contamination levels in excess of that expected from extrapolation of Eq. (1) can occur during processing at these moderate temperatures. One study found up to $\sim 10^{12}$ cm^{-3} of iron incorporated at 650 °C which had the effect of reducing minority carrier lifetime in high-quality material down to a few tens of microseconds [11]. The iron concentration in this study is broadly in agreement with the data presented here. Equation (2) represents a parameterisation of the degree to which enhanced iron contamination can occur below ~ 800 °C. It explains why improved surface cleaning methods were necessary for processes performed at these lower temperatures [11]. Furthermore, it is noted that long low-temperature anneals are less effective above ~ 600 °C [9], which could be explained by enhanced iron solubility.

5 Summary As one of the most detrimental impurities in silicon, it is vital to understand the solubility of iron as a function of temperature. We have measured the degree to which iron can dissolve in silicon below ~ 800 °C and find it to be substantially enhanced when compared to an extrapolation of established higher temperature data. The magnitude of this enhancement can be a factor of >20 at 600 °C. This explains why substantial reductions in minority carrier lifetime have been measured after processing at such temperatures.

Figure 3 Iron concentrations in Czochralski silicon samples contaminated at different temperatures in air. The dotted line is the high temperature iron solubility from Istratov et al. [10]. The open symbol is for a sample pre-annealed at 720 °C.

References

[1]   S. M. Myers et al., J. Appl. Phys. **88**, 3795 (2000).
[2]   G. Coletti et al., Adv. Funct. Mater. **21**, 879 (2011).
[3]   A. A. Istratov et al., Appl. Phys. A **70**, 489 (2000).
[4]   S. Rein and S. W. Glunz, J. Appl. Phys. **98**, 113711 (2005).
[5]   D. P. Fenning et al., Appl. Phys. Lett. **98**, 162103 (2011).
[6]   A. F. B. Braga et al., Sol. Energy Mater. Sol. Cells **92**, 418 (2008).
[7]   S. P. Phang and D. Macdonald, J. Appl. Phys. **109**, 073521 (2011).
[8]   K. J. Fraser et al., Mater. Sci. Eng. B **159/160**, 194 (2009).
[9]   M. Rinio et al., Prog. Photovolt.: Res. Appl. **19**, 165 (2011).
[10] A. A. Istratov et al., Appl. Phys. A **69**, 13 (1999).
[11] R. Falster and G. Borionetti, ASTM STP **1340**, 226 (1998).
[12] G. Zoth and W. Bergholz, J. Appl. Phys. **67**, 6764 (1990).
[13] R. A. Sinton and A. Cuevas, Appl. Phys. Lett. **69**, 2510 (1996).
[14] W. Wijaranakula, J. Electrochem. Soc. **140**, 275 (1993).
[15] J. D. Murphy et al., J. Appl. Phys., in press, DOI: 10.1063/1.3632067 (2011).
[16] S. A. McHugo et al., Appl. Phys. Lett. **73**, 1424 (1998).